Biophysical Journal
Article

Biophysical Society

Effects of Modified Parvalbumin EF-Hand Motifs on Cardiac Myocyte Contractile Function

Michelle L. Asp,[1] Frances V. Sjaastad,[1] Jalal K. Siddiqui,[2] Jonathan P. Davis,[2] and Joseph M. Metzger[1,*]
[1]Department of Integrative Biology and Physiology, University of Minnesota Medical School, Minneapolis, Minnesota; and [2]Department of Physiology and Cell Biology, The Ohio State University College of Medicine, Columbus, Ohio

ABSTRACT Cardiac gene delivery of parvalbumin (Parv), an EF-hand Ca^{2+} buffer, has been studied as a therapeutic strategy for diastolic heart failure, in which slow Ca^{2+} reuptake is an important contributor. A limitation of wild-type (WT) Parv is the significant trade-off between faster relaxation and blunted contraction amplitude, occurring because WT-Parv sequesters Ca^{2+} too early in the cardiac cycle and prematurely truncates sarcomere shortening in the facilitation of rapid relaxation. We recently demonstrated that an E → Q substitution (ParvE101Q) at amino acid 12 of the EF-hand Ca^{2+}/Mg^{2+} binding loop disrupts bidentate Ca^{2+} binding, reducing Ca^{2+} affinity by 99-fold and increasing Mg^{2+} affinity twofold. ParvE101Q caused faster relaxation and not only preserved contractility, but unexpectedly increased it above untreated myocytes. To gain mechanistic insight into the increased contractility, we focused here on amino acid 12 of the EF-hand motif. We introduced an E → D substitution (ParvE101D) at this site, which converts bidentate Ca^{2+} coordination to monodentate coordination. ParvE101D decreased Ca^{2+} affinity by 114-fold and increased Mg^{2+} affinity 28-fold compared to WT-Parv. ParvE101D increased contraction amplitude compared to both untreated myocytes and myocytes with ParvE101Q, with limited improvement in relaxation. Additionally, ParvE101D increased spontaneous contractions after pacing stress. ParvE101D also increased Ca^{2+} transient peak height and was diffusely localized around the Z-line of the sarcomere, suggesting a Ca^{2+}-dependent mechanism of enhanced contractility. Sarcoplasmic reticulum Ca^{2+} load was not changed with ParvE101D, but postpacing Ca^{2+} waves were increased. Together, these data show that inverted Ca^{2+}/Mg^{2+} binding affinities of ParvE101D increase myocyte contractility through a Ca^{2+}-dependent mechanism without altering sarcoplasmic reticulum Ca^{2+} load and by increasing unstimulated contractions and Ca^{2+} waves. ParvE101D provides mechanistic insight into how changes in the Ca^{2+}/Mg^{2+} binding affinities of parvalbumin's EF-hand motif alter function of cardiac myocytes. These data are informative in developing new Ca^{2+} buffering strategies for the failing heart.

INTRODUCTION

Parvalbumin (Parv) is a cytosolic calcium (Ca^{2+}) buffering protein endogenously expressed in glycolytic skeletal muscle, where it facilitates fast relaxation (1). Wild-type Parv (WT-Parv) contains two functional EF-hand metal ion binding sites, the CD domain and the EF domain, that bind Ca^{2+} with high affinity (~10^{-8} M) and Mg^{2+} with moderate affinity (~10^{-4} M) (2). Because basal cytosolic Ca^{2+} and Mg^{2+} concentrations are ~10–100 nM and 1 mM, respectively, WT-Parv binds Mg^{2+} almost exclusively at rest (2). When an action potential triggers Ca^{2+} release from the sarcoplasmic reticulum (SR), Mg^{2+} must first dissociate from Parv before Ca^{2+} can bind. This delay in Ca^{2+} binding allows for contraction to occur before Ca^{2+} is buffered by Parv (2).

Canonical EF-hand motifs consist of a helix-loop-helix structure, where divalent metal cations coordinate with oxygen atoms of highly conserved amino acids in the 12-residue loop region. Coordinating oxygen atoms are from loop residues 1, 3, 5, 7, 9, and 12 (3,4). The two EF-hand binding loops in WT-Parv are able to discriminate between the chemically similar Mg^{2+} and Ca^{2+} ions because of their difference in size and preferred coordination states. Six coordinating oxygen atoms in an octahedral configuration are optimal for Mg^{2+} binding, whereas seven coordinating oxygen atoms in a pentagonal bipyrimidal configuration are optimal for Ca^{2+} (4,5). The highly conserved glutamate at position 12 of the EF-hand loop provides monodentate coordination with one side-chain oxygen atom when Mg^{2+} is bound and bidentate coordination with both available oxygen atoms when Ca^{2+} is bound (4). Thus, EF-hand motif residue 12 is key for divalent cation selectivity (4,6). The ability of the EF-hands in WT-Parv to

Submitted January 22, 2016, and accepted for publication March 31, 2016.
*Correspondence: metzgerj@umn.edu
Editor: David Warshaw.
http://dx.doi.org/10.1016/j.bpj.2016.03.037

accommodate either Ca^{2+} or Mg^{2+} ions is what confers its unique function as a delayed Ca^{2+} buffer to increase the relaxation rate in fast-twitch muscle.

The therapeutic potential of transient intracellular Ca^{2+} buffering for diastolic dysfunction in the heart has been investigated because delayed Ca^{2+} reuptake is an important contributor to slow or incomplete relaxation in diseased myocardium (7). Ca^{2+} buffering in the heart has been tested by adenoviral gene transfer of WT-Parv in isolated cardiac myocytes because Parv is not expressed endogenously in the heart (8). These experiments demonstrated that Parv-expressing myocytes have a significantly faster relaxation rate, but this occurs at the expense of blunted contractile function (9). Reduced contraction amplitude was attributed to the kinetics of WT-Parv, which are optimized for the short bursts of contraction/relaxation cycling that occur in fast-twitch muscle. In the context of the cardiac myocyte, WT-Parv binds Ca^{2+} too early in the contractile cycle, which decreases Ca^{2+} binding to the myofilaments and subsequently blunts contraction (10). To optimize the kinetics of Ca^{2+} buffering for the human heart, it was hypothesized that a modified delayed buffer, engineered with decreased Ca^{2+} and/or increased Mg^{2+} binding affinities, would be required (11,12).

We recently demonstrated that substituting a glutamine for the highly conserved glutamate at the 12th amino acid of the EF-hand ion binding loop of carp β-Parvalbumin (ParvE101Q) decreased Ca^{2+} affinity by 99% and paradoxically increased Mg^{2+} affinity twofold compared to WT-Parv (13). This E → Q substitution eliminated the bidentate coordination required for optimal Ca^{2+} binding in the EF-hand loop. The combination of decreased Ca^{2+} affinity and increased Mg^{2+} affinity in ParvE101Q further delayed Ca^{2+} buffering relative to WT-Parv, enabling ParvE101Q to be more optimally designed for the human heart (13). One unexpected observation in these experiments was that ParvE101Q not only preserved contractile function, because of the delayed Ca^{2+} buffering, but also increased contraction amplitude 24% above untreated myocytes (13). This is in stark contrast to the severe diminution of contraction amplitude characteristic of WT-Parv (9). The basis for the heightened contractile function of ParvE101Q is not known. One hypothesis is that localized Mg^{2+} buffering, together with increased Mg^{2+} affinity of ParvE101Q, accounts in part for this effect (13).

To accomplish the goal of implementing a Ca^{2+} buffering system into diseased cardiac muscle, a deeper understanding of EF-hand motifs is required in the context of the cardiac myocyte and its unique excitation-contraction pathway. Specifically, it is imperative to understand how a Ca^{2+} buffering protein such as ParvE101Q could, paradoxically, increase myocyte contractility. To gain mechanistic insight into the increase in contractility found with ParvE101Q, we focused here on the 12th amino acid of the canonical EF-hand motif. Another EF-hand loop residue 12 substitution that has been studied from a structural standpoint is ParvE101D (6,14). Although glutamate at position 12 of the metal ion binding loop of canonical EF-hands is highly conserved, ~8% of EF-hand motifs contain an aspartate at this position (4). Substitution of glutamate for aspartate at the 12th residue of the EF-hand ion binding loop in carp β-parvalbumin resulted in monodentate Ca^{2+} binding and an even more drastic inversion of Ca^{2+} and Mg^{2+} binding affinities than ParvE101Q (6,13). The effects of ParvE101D on intact cardiac myocyte mechanical function and Ca^{2+} handling have not been tested. If the inverted Ca^{2+}/Mg^{2+} binding affinities of ParvE101Q have a mechanistic role in increasing contraction amplitude, ParvE101D should elicit similar or greater effects in terms of enhanced contractility.

The purpose of this study was therefore to test the hypothesis that inverted Ca^{2+}/Mg^{2+} binding affinities in ParvE101D increase contractile function in cardiac myocytes. The results of these experiments provide evidence that the increased Mg^{2+} affinity and decreased Ca^{2+} affinity of ParvE101D increases contractile function and gives new mechanistic insight into enhanced contractility at the subcellular level. Additionally, the data presented here increase knowledge of how specific structural changes in EF-hand motifs underlie functional effects in cardiac myocyte physiology, particularly related to changes in coordination spheres for divalent metal ions. This work provides the critical framework to optimize this protein-based transient Ca^{2+} buffering strategy for human heart failure.

MATERIALS AND METHODS

Ca^{2+}/Mg^{2+} affinity and dissociation rates

The Ca^{2+} and Mg^{2+} affinities and dissociation rates were measured at 35°C in bacterially expressed and purified proteins as previously described (12,13). Briefly, all steady-state fluorescence measurements were performed using a Perkin-Elmer LS55B Spectrofluorometer (Waltham, MA) by adding microliter amounts of $CaCl_2$ or $MgCl_2$ to 2 ml of the proteins (1 μM) in 200 mM 3-(*N*-morpholino)propanesulfonic acid, 150 mM KCl, 4 mM EGTA, 1 mM DTT, pH 7.0. Ca^{2+} and Mg^{2+} dissociation rates were measured using an Applied Photophysics (Leatherhead, UK) model SX.18 MV stopped-flow instrument. The buffer used for the stopped-flow experiments was 10 mM 3-(*N*-morpholino)propanesulfonic acid, 150 mM KCl, 1 mM DTT, at pH 7.0.

Adenovirus production

Human α-parvalbumin recombinant DNA was subcloned into the TOPO TA vector system (Life Technologies, Grand Island, NY), transformed into One Shot TOP10 chemically competent *Escherichia coli* (Life Technologies), and ligated into the pDC316 plasmid (Microbix Biosystems, Mississauga, Ontario, Canada). Amino acid substitutions were incorporated using the QuikChange II XL Site-Directed Mutagenesis Kit (Agilent Technologies, Santa Clara, CA) and DNA transformed into XL1 Blue Supercompetent Cells (Agilent). Sequence-verified clones were used for making adenovirus.

The F102W substitution was incorporated into all parvalbumins to conduct in vitro fluorescence binding assays. This substitution does not significantly alter Ca^{2+}/Mg^{2+} binding affinities compared to WT-Parv (13), so ParvF102W was used as a positive control for our experiments.

Another substitution, D51A was incorporated to disable ion binding in the CD site, as shown previously (13,14), to simplify Parv structure-function analysis. ParvE101D and ParvE101Q contain all three substitutions. As a negative control, an inactive Parv with disabled cation binding in both the CD and EF hands was developed by incorporating three substitutions—D53N, D90A, and F102W. These three substitutions were previously shown to eliminate Ca^{2+} and Mg^{2+} binding (13). A FLAG tag (DYKDDDDK) was inserted onto the N-terminal end of all Parvs because the F102W substitution prevents Western blot and IF detection by commercially available antibodies. Fig. 1 shows the amino acid substitutions included in each construct (Fig. 1 *A*) and illustrates the loss of the seventh coordinating oxygen for Ca^{2+} binding in the EF ion binding site with ParvE101D and ParvE101Q (Fig. 1 *B*).

Adenovirus was made using the Ad-Max Adenoviral Vector System (Microbix Biosystems). 293 cells underwent calcium phosphate transfection (15) with pDC316-Parv and pBHGloxΔE1,E3, followed the next day by noble agar overlay. Plaques were harvested, expanded, and adenovirus purified using the AdenoX Maxi Purification Kit (Clontech Laboratories, Mountain View, CA), or high-titer purified virus was made by the University of Michigan Vector Core.

Adult rat cardiac myocyte isolation and culture

Cardiac myocytes from adult female Sprague-Dawley rats (Harlan Laboratories, Indianapolis, IN) were isolated and cultured as previously described (16). Myocytes were plated on laminin coated glass coverslips at a density of 20,000 cells/coverslip. 1 h after plating, myocytes were treated with adenovirus in modified M199 medium (Gibco, Life Technologies, Grand Island, NY) containing 26 mM $NaHCO_3$, 25 mM Hepes, 0.2% (w/v) bovine serum albumin, 1% (v/v) ITS (insulin, transferrin, sodium selenite, Sigma Aldrich, St. Louis, MO), and 1× Penicillin/Streptomycin. Myocytes were given fresh media the next morning. Experiments were done 3 days post-gene transfer. Myocytes were maintained in culture at 37°C and 5% CO_2.

Western blotting and immunofluorescence

Relative Parv expression was determined by sodium dodecyl sulfate-polyacrylamide gel electrophoresis and Western blotting of protein from virus-treated myocytes. Briefly, protein was boiled in radio-immunoprecipitation assay buffer with 2× Laemmli buffer and protease inhibitors for 5 min and then separated by sodium dodecyl sulfate-polyacrylamide gel electrophoresis on a 4–12% bis-tris gel (NuPAGE, Life Technologies). Protein was transferred to a PVDF membrane, blocked with 5% nonfat dry milk, and blotted with FLAG M2 mouse monoclonal antibody (1:1,500; Sigma F1804) and actin N-term rabbit polyclonal antibody (1:15,000; Sigma A2013) overnight at 4°C. The next day, membranes were incubated with secondary antibodies (goat antimouse IRDye 680, 1:10,000, LiCOR, Lincoln NE; and goat antirabbit IRDye 800, 1:10,000, Rockland Immunochemicals, Limerick, PA) for 1 h at room temperature. Membranes were imaged on the LiCOR Odyssey Infrared Imaging System.

Immunofluorescence detection of ParvE101D was done to determine subcellular localization. Myocytes were fixed in 4% paraformaldehyde, permeabilized with Triton X-100, and blocked with 20% normal goat serum (NGS). Myocytes were probed with FLAG M2 (1:500) and actin N-term (1:1000) for 1 h in 2% NGS. Myocytes were washed, reblocked in 2% NGS and probed with antimouse AF488 (1:500) and antirabbit 594 (1:1000). Coverslips were mounted onto slides with Permafluor mounting medium (Thermo Scientific, Waltham, MA) and imaged on a Zeiss Axioskop LSM 510 laser scanning confocal microscope (Thornwood, NY).

Sarcomere length measurements

Contraction and relaxation kinetics were measured with the Myocyte Calcium and Contractility System by IonOptix (Milton, MA) 3 days after adenovirus treatment. Myocytes were bathed in Tyrode's solution and stimulated at 0.2 or 1 Hz and 25 V. For the pacing stress experiment, myocytes were paced for 20 s each at 0.2, 0.5, 1.0, and 2.0 Hz, after which pacing was stopped and spontaneous contractions were recorded for 20 s. To test acute changes in Mg^{2+}, untreated myocytes 1 day postisolation were used. Myocytes were paced for 2 min at 0.2 Hz in Tyrode's containing 0.2, 0.8, or 5.0 mM Mg^{2+}, after which sarcomere length measurements were recorded for 10 min. Myocytes were visualized using an inverted microscope (Nikon Eclipse TE2000-U, Melville, NY) with a 40× objective. Sarcomere length data were acquired at 1000 Hz. Contractions were averaged and analyzed with IonWizard software (IonOptix) using fast Fourier transform. All experiments were carried out at 30°C.

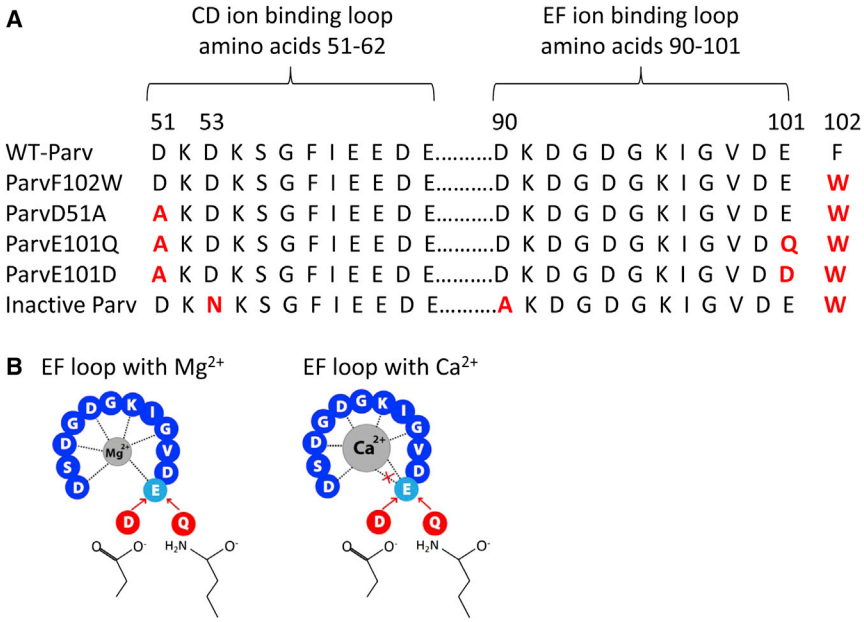

FIGURE 1 Amino acid substitutions in human α-parvalbumin. (*A*) Amino acid sequences of the CD and EF metal ion binding loop of human α-Parv. Red letters represent substituted amino acids for each of the modified proteins. (*B*) Schematic representation of the EF-hand Ca^{2+}/Mg^{2+} binding loop. Dotted lines represent amino acids providing coordinating oxygen atoms. The six coordinating oxygen atoms preferred by Mg^{2+} are available with E, D, or Q at residue 101. The seven oxygen atoms preferred by Ca^{2+} can only occur with bidentate coordination of E at residue 101. Substituting D or Q eliminates the seventh coordinating oxygen when Ca^{2+} is bound.

Calcium measurements

Calcium transients

Myocytes were loaded with 2 μM Fura-2AM (Life Technologies) for 10 min, followed by deesterification for 20 min at room temperature. Calcium transient data were collected with the IonOptix Myocyte Calcium and Contractility System, using the μ-Stepper Switch to measure 360 nm:380 nm, which gives the relative change in cytosolic Ca^{2+}. 360 nm measures both Ca^{2+} bound and Ca^{2+}-free Fura, and 380 nm measures Ca^{2+}-free Fura. The 380 nm wavelength is measured at 1000 Hz, and the 360 nm wavelength measured once every 10 s to account for any photobleaching or loss of Fura. Cells were paced at 0.2 or 1.0 Hz and 25 V at 30°C, transients were averaged, and kinetics calculated using IonWizard Software.

SR calcium load

SR Ca^{2+} load was measured by treating cells with caffeine and measuring the 340:380 nm ratio using the Ionoptix system fitted with the HyperSwitch, which measures Ca^{2+} bound (340 nm) and Ca^{2+}-free (380 nm) Fura at 250 Hz in real time (no extrapolation of wavelengths is required). Myocytes were loaded with Fura-2 AM for 5 min, followed by 10 min deesterification, and then mounted onto a heated perfusion chamber. Myocytes were first perfused with normal Tyrode's and paced for ~10 contractions. The perfusate was then switched to Ca^{2+}-free, Na^{+}-free Tyrode's for ~20 s, followed by perfusion with Ca^{2+}-, Na^{+}-free Tyrode's with 20 mM caffeine for 8 s. Caffeine was washed out with Ca^{2+}-free, Na^{+}-free Tyrode's and finally, cells were paced again with normal Tyrode's at the end of the experiment to ensure cells were still viable and Ca^{2+} cycling was intact. Li^{+} was used to replace Na^{+} in the Ca^{2+}/Na^{+}-free solution. One myocyte was analyzed per coverslip.

Calcium sparks

Myocytes were loaded with 10 μM Fluo-4AM (Life Technologies) for 20 min and deesterification proceeded for another 20 min at room temp. Myocytes were bathed in Tyrode's solution and viewed with a 63× oil objective on a Zeiss Axioskop LSM 510 laser scanning confocal microscope, and sparks were measured with the line scanning feature using an argon laser with excitation at 488 nm and fluorescence measured at >505 nm. A single line of 512 pixels was scanned 1000 times, with a 1.61 μsec/pixel dwell time, pixel size of 0.3 μm, and 3.07 msec/line scanning speed, at 30°C after 20 s of pacing at 1 Hz. Sparks were analyzed using the SparkMaster plugin (17) for Image J (National Institutes of Health, Bethesda, MD). The criteria were set at 3.8 for all myocytes.

Statistical analysis

Data were analyzed using GraphPad Prism 6 (La Jolla, CA). For most experiments, a two-tailed *t*-test was used to measure differences between two groups and one-way analysis of variance with Tukey's test for multiple comparisons was used to compare more than two groups. A Mann-Whitney test was used to analyze Ca^{2+} sparks because the data were not normally distributed. Spontaneous contractions were analyzed with a Chi-square test, and Ca^{2+} waves were analyzed with a Fisher's exact test. $P < 0.05$ was considered statistically significant.

RESULTS

Ca^{2+}/Mg^{2+} binding affinities and dissociation rates

In vitro experiments with purified ParvF102W and ParvE101D were conducted to determine the Ca^{2+} and Mg^{2+} binding affinities and dissociation rates in the context of the human α-parvalbumin isoform. This isoform was studied to allow for more relevant translation in potential future clinical applications. These experiments revealed a 114-fold decrease in Ca^{2+} affinity and a 28-fold increase in Mg^{2+} affinity for ParvE101D compared to ParvF102W. Dissociation rates were 95% faster for Ca^{2+} and 95% slower for Mg^{2+} in ParvE101D compared to ParvF102W (Table 1). Compared to published data for carp β-ParvE101Q, human α-ParvE101D has a slightly lower Ca^{2+} affinity and a notably larger increase in Mg^{2+} affinity, twofold versus 28-fold over ParvF102W (13).

Myocyte contraction studies

To determine the functional effects of modified Parvs, adult rat cardiac myocytes underwent adenoviral gene transfer to induce Parv expression and then sarcomere length measurements were made. Protein expression is illustrated in Fig. 2 *A*. ParvF102W was used as a positive control because it has been shown to have similar Ca^{2+}/Mg^{2+} binding affinities and contractility/relaxation effects as WT-Parv (13). ParvD51A was tested to determine the effect of disabling ion binding in the Parv CD loop. Compared to untreated myocytes, both ParvF102W and ParvD51A exhibited diminished contraction amplitude (Fig. 2, *B* and *C*), and had faster times from peak to 25% and 50% relaxation (Fig. 2, *B* and *D*). The 75% relaxation time for ParvD51A was not different from untreated myocytes (Fig. 2, *B* and *D*), indicating a decreased buffering capacity in the late relaxation phase by disabling the CD loop. Together, these data demonstrate that ParvF102W has a similar effect compared to previously published data on WT-Parv (9), and disabling the CD site does not appreciably alter contraction or early relaxation compared to ParvF102W at the expression levels in this experiment.

In contrast to ParvF102W and ParvD51A, equal protein expression of ParvE101D (Fig. 2 *A*) resulted in significantly increased contraction amplitude (Fig. 2, *B* and *C*), and had no significant effect on relaxation (Fig. 2, *B* and *D*). Additionally, time from baseline to peak height (*peak time*)

TABLE 1 Ca^{2+}/Mg^{2+} Binding Affinities and Dissociation Rates for Human α-ParvF102W and E101D

	ParvF102W	ParvE101D
Binding Sites	2[a]	1[a]
Ka^{Ca2+} (M^{-1})	$5 \times 10^8 \pm 1 \times 10^8$	$4.4 \times 10^6 \pm 0.1 \times 10^6$
Ka^{Mg2+} (M^{-1})	$3.243 \times 10^4 \pm 0.008 \times 10^4$	$9 \times 10^5 \pm 2 \times 10^5$
Kd^{Ca2+} (nM)	2.4 ± 0.5	226 ± 7
Kd^{Mg2+} (μM)	30.84 ± 0.08	1.4 ± 0.3
K_{off}^{Ca2+} (S^{-1})	1.81 ± 0.06	31.5 ± 0.8
K_{off}^{Mg2+} (S^{-1})	13.4 ± 0.4	1.36 ± 0.01
K_{on}^{Ca2+} ($M^{-1}S^{-1}$)	$8 \times 10^8 \pm 2 \times 10^8$	$1.40 \times 10^8 \pm 0.05 \times 10^8$
K_{on}^{Mg2+} ($M^{-1}S^{-1}$)	$4.4 \times 10^5 \pm 0.1 \times 10^5$	$10 \times 10^5 \pm 2 \times 10^5$

[a]Not directly tested in this experiment, but inferred from data in (13).

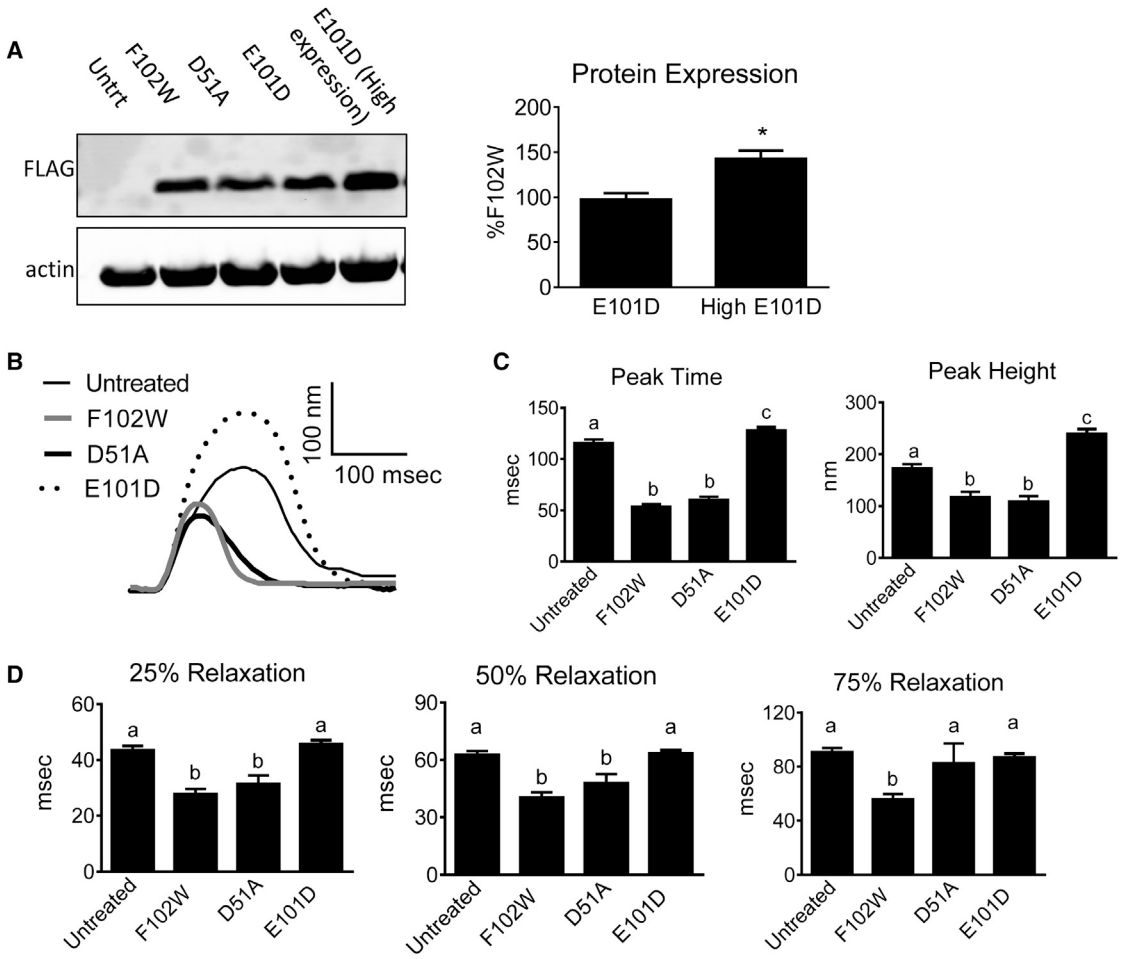

FIGURE 2 Protein expression and contractile function of ParvF102W, ParvD51A, and ParvE101D. (*A*) Left: Western blot showing relative expression levels of ParvF102W, D51A, and E101D. Untrt, untreated myocytes. Right: Quantification of band density for low and high ParvE101D expression, normalized to actin and expressed as a percentage of ParvF102W on the same blot. Bars are mean ± SE of bands from 11 to 12 samples from seven rats. $*P < 0.05$. (*B*) Representative traces normalized to baseline, and (*C*) contraction and (*D*) relaxation function of untreated myocytes and myocytes expressing equal protein expression of ParvF102W, D51A, and E101D. Relaxation was measured as time from peak height. Myocytes were paced at 0.2 Hz and 30°C. Data are presented as mean ± SE, $N = 27–55$ myocytes/group from four rats. Groups with different letters have $P < 0.05$.

was increased with ParvE101D (Fig. 2 *B*). The absence of an effect on relaxation suggests minimal Ca^{2+} buffering occurs with ParvE101D at this level of protein expression.

Because increasing intracellular Parv concentration increases Ca^{2+} buffering capacity (18), the effect of increased expression of ParvE101D was tested. A relative 1.5-fold increase in ParvE101D protein expression (Fig. 2 *A*, *high expression*) caused a significant increase in contraction amplitude compared to untreated myocytes (Fig. 3, *A* and *B*), and also exhibited decreased time from peak to 75% relaxation (Fig. 3, *A* and *C*). These data suggest the presence of Ca^{2+} buffering in the late relaxation phase with high expression of ParvE101D, although this did not translate to a shorter duration of the entire contraction/relaxation cycle because of the increased peak time (Fig. 3, *A* and *B*). When compared to human α-ParvE101Q, ParvE101D had significantly greater contraction amplitude and slower relaxation. The effects of human α-ParvE101Q closely mirror the effects of carp β-ParvE101Q previously published (13). The functional differences between ParvE101D and ParvE101Q suggest that higher Mg^{2+} affinity and slower Mg^{2+} dissociation from ParvE101D may have an important role in both the peak height of contraction and the timing of Ca^{2+} buffering. Corroborating this finding, increasing the pacing rate from 0.2 to 1 Hz preserved the increased contraction amplitude but abrogated the relaxation effect in ParvE101D-treated myocytes (Fig. 3 *D*).

Several additional experiments were performed to mechanistically dissect the increased contraction amplitude caused by ParvE101D. First, it was noted that ParvE101D sensitized myocytes to spontaneous contractions in unstimulated conditions. To quantify this effect, myocytes underwent pacing stress after which spontaneous contractions were counted (Fig. 4 *A*). In the 20 s immediately following pacing, myocytes expressing ParvE101D had a significantly

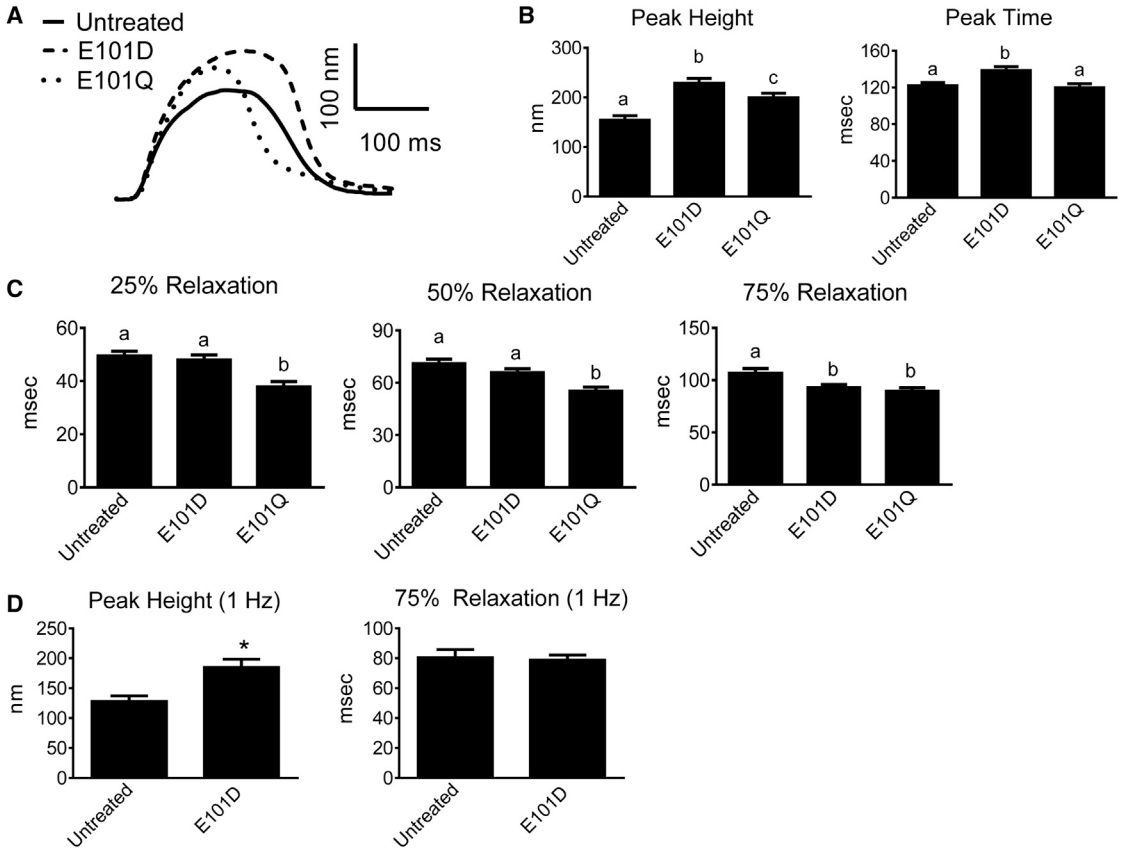

FIGURE 3 Function of ParvE101D compared with ParvE101Q. (*A*) Representative traces normalized to baseline, and (*B*) contraction and (*C*) relaxation function of untreated myocytes and myocytes treated with ParvE101D and ParvE101Q. Relaxation is measured as time from peak height. Data were collected at 0.2 Hz and 30°C. $N = 56–57$ myocytes/group from four rats. Different letters have $P < 0.05$. (*D*) Peak height and 75% relaxation time for untreated myocytes and myocytes with ParvE101D paced at 1 Hz and 30°C. $N = 52–56$ myocytes per group from three rats, $*P < 0.05$. All data are presented as mean ± SE.

higher number of spontaneous contractions (Fig. 4 *B*). Second, to determine the necessity of Ca^{2+}/Mg^{2+} binding for the increased contractility of ParvE101D, myocytes expressing an inactive Parv (both CD and EF cation binding loops disabled) were tested. At expression levels causing robust effects in myocytes expressing ParvF102W and ParvE101D (Fig. 4 *C*), the inactive Parv had no effect on contraction amplitude (Fig. 4 *D*), indicating that cation binding is necessary for the increased contractile function of ParvE101D. Finally, myocytes acutely treated with buffer containing high and low Mg^{2+} concentrations exhibited decreased and increased contraction amplitude, respectively (Fig. 4 *E*). The Mg^{2+} dependence on contractile function in this experiment provides indirect evidence that the Mg^{2+} buffering capacity of ParvE101D may have a mechanistic role in increasing contraction.

Calcium transients

To further probe the mechanism of increased contractility in ParvE101D, Ca^{2+} transients were measured in myocytes loaded with Fura-2 AM. Compared to untreated myocytes, ParvE101D-expressing myocytes had a significant increase in Ca^{2+} transient amplitude and a faster time from peak to 75% Ca^{2+} transient decay (Fig. 5, *A–C*). ParvE101Q also caused increased peak Ca^{2+} transient amplitude and faster times from peak to 50% and 75% decay (Fig. 5, *A–C*), indicating ParvE101Q buffers Ca^{2+} earlier in the relaxation phase than ParvE101D. When ParvE101D-treated myocytes were paced at 1 Hz, peak Ca^{2+} transient amplitude remained significantly increased, but faster decay was no longer evident (Fig. 5 *D*), indicating that Ca^{2+} binding by ParvE101D is too delayed to buffer Ca^{2+} at a higher pacing rate. Taken together, the Ca^{2+} transient data closely mirror the contractility data, suggesting that both the contraction and relaxation effects of human α-ParvE101D and α-ParvE101Q are occurring through a Ca^{2+}-dependent mechanism.

Subcellular localization

Immunofluorescence imaging of ParvE101D expression in cardiac myocytes was done to determine if subcellular localization could provide insight into the increased contractile

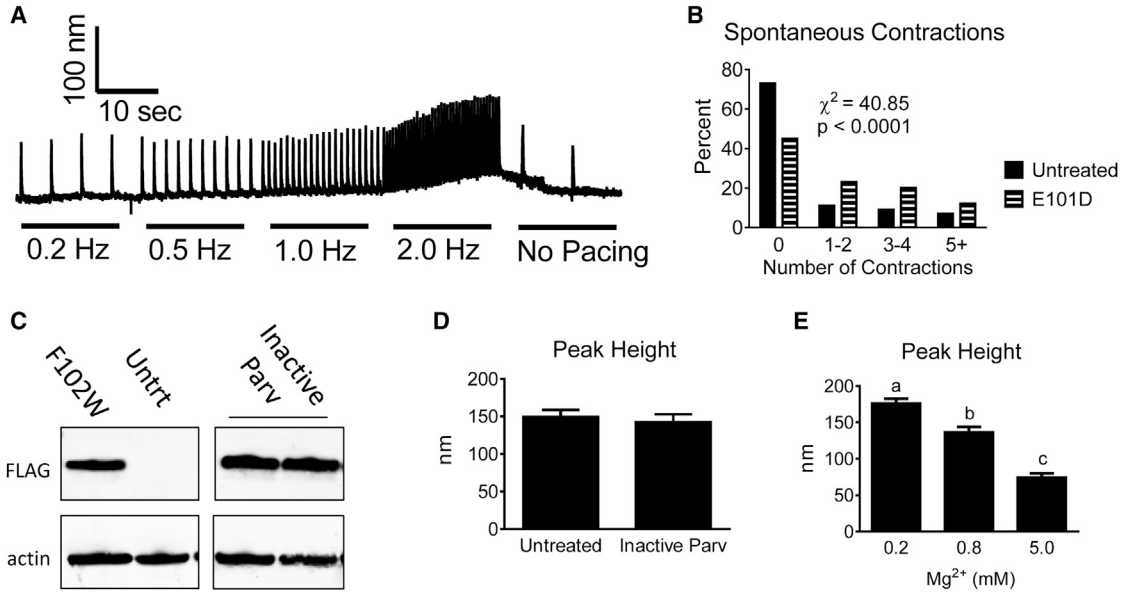

FIGURE 4 Spontaneous contractions with ParvE101D, Inactive Parv contractile function, and function of myocytes with acute changes in Mg^{2+}. (*A*) Representative trace and (*B*) histogram depicting the percentage of myocytes having unstimulated contractions after a pacing stress protocol. $N = 56–60$ myocytes/group from six rats. Untreated and ParvE101D groups are significantly different from each other. (*C*) Protein expression of Inactive Parv in cardiac myocytes 3 days after viral gene transfer. All bands are on the same blot, but intervening lanes were omitted. Untrt, untreated myocytes. (*D*) Peak height of cardiac myocytes expressing Inactive Parv. Data were collected at 0.2 Hz, and $N = 36–41$ myocytes per group from three rats. (*E*) Peak height was measured in cardiac myocytes acutely treated with varying concentrations of extracellular Mg^{2+} at 0.2 Hz. $N = 51–53$ myocytes from three rats. Different letters have $P < 0.05$. All experiments were done at 30°C.

function and Ca^{2+} transient amplitude. Myocytes were fixed and then permeabilized before treating with antibodies against FLAG (for ParvE101D detection) and actin. Confocal microscopy revealed general diffuse ParvE101D staining throughout myocytes, and a striated pattern that colocalized between the actin striated pattern (Fig. 6 *A*). When myocytes were permeabilized, washed, and then probed for ParvE101D via Western blot, there was no detectable band (Fig. 6 *B*), indicating that ParvE101D is cytosolic and weakly associated with the Z-line of the sarcomere.

SR Ca^{2+} load and Ca^{2+} leak

Increased Ca^{2+} transients caused by ParvE101D and its weak localization with the Z-line suggested that ParvE101D may affect the process of calcium-induced calcium release (CICR). Increased Ca^{2+} transients can occur as a result of increased SR Ca^{2+} load and/or increasing the percentage of total SR Ca^{2+} released through RyR2 during CICR (19). Thus, functional SR Ca^{2+} load was measured by caffeine treatment of myocytes, without Ca^{2+} and Na^{+} to eliminate potential confounding effects of NCX activity (20) (Fig. 7 *A*). Compared to untreated myocytes, ParvE101D-expressing myocytes had no increase in the peak height of the Ca^{2+} transient with caffeine (Fig. 7 *B*). Because of the increase in spontaneous contractions with ParvE101D (Fig. 4 *B*), Ca^{2+} sparks were measured to determine whether ParvE101D affects RyR2 open probability (Fig. 7 *C*). In myocytes expressing ParvE101D, there was no difference in spark frequency or amplitude (Fig. 7 *D*). Interestingly, the number of Ca^{2+} waves was increased with ParvE101D (Fig. 7, *C* and *E*), providing mechanistic insight into the spontaneous contractions measured in Fig. 4. Taken together, these data suggest that increased Ca^{2+} transients caused by ParvE101D are occurring independently of increased SR Ca^{2+} load. Despite no difference in Ca^{2+} spark frequency, increased Ca^{2+} waves suggests a potential role for ParvE101D to induce alterations in Ca^{2+} cycling.

DISCUSSION

This study provides new, to our knowledge, mechanistic insights into the biophysical effects of parvalbumin-based modified EF-hand motifs. We tested the hypothesis that the inverted Ca^{2+}/Mg^{2+} binding affinities of ParvE101D will increase contractility in cardiac myocytes. The main new findings from this study are 1) the 114-fold lower Ca^{2+} affinity and 28-fold higher Mg^{2+} affinity of ParvE101D compared with ParvF102W led to significant increases in Ca^{2+} transient amplitude and decreased time to 75% transient decay, 2) Ca^{2+} transient alterations can explain the increased contraction amplitude and decreased time to 75% relaxation, 3) increased contractility by ParvE101D was greater than ParvE101Q, and 4) altered global Ca^{2+} handling by ParvE101D caused an increase in

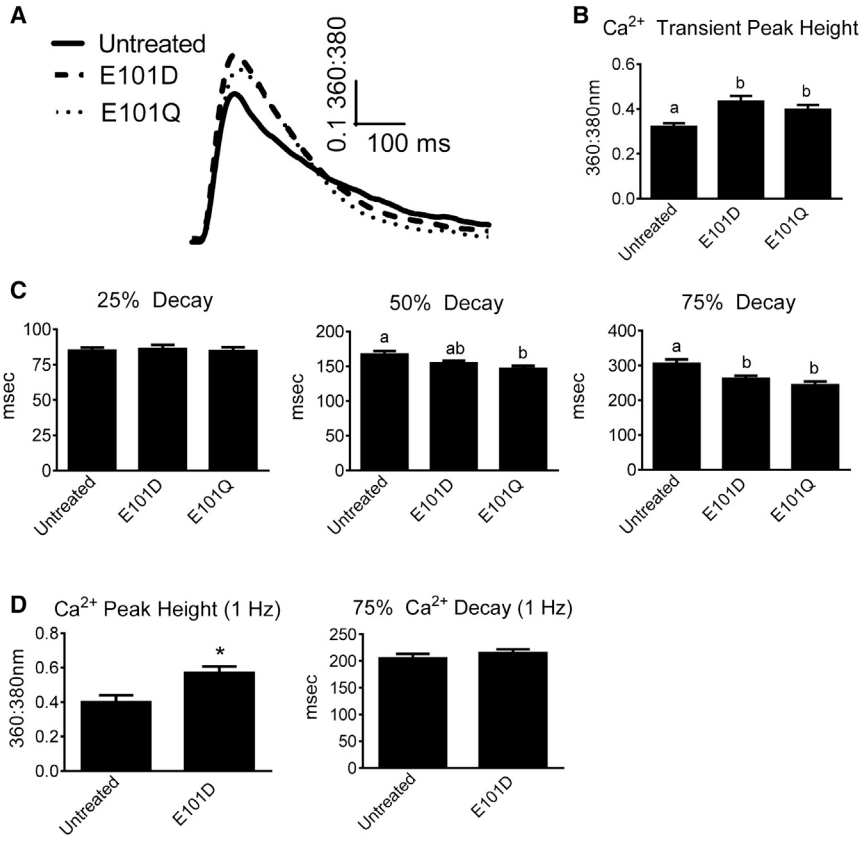

FIGURE 5 Ca^{2+} transients from myocytes with ParvE101D and ParvE101Q. Myocytes were loaded with Fura-2 AM and 360:380 nm was measured to determine the relative amount of intracellular Ca^{2+}. (*A*) Representative traces, and (*B*) transient peak, and (*C*) decay kinetics for untreated myocytes and myocytes with ParvE101D or ParvE101Q. Myocytes were paced at 0.2 Hz and 30°C. $N = 56–57$ myocytes/group from four rats. Different letters have $P < 0.05$. (*D*) Transient peak and decay for untreated myocytes and myocytes with ParvE101D paced at 1 Hz and 30°C. $N = 35–39$ myocytes per group from three rats. Data are presented as mean ± SE, $^*P < 0.05$ compared to untreated cells.

spontaneous Ca^{2+} waves. The knowledge gained from these experiments provides new insight into the complexities of altered Ca^{2+} and Mg^{2+} binding affinities and dissociation rates of modified parvalbumins in the regulation of contractile function in living cardiac myocytes. These data further highlight the importance of parvalbumin's EF-hand loop residue 12 in conferring Ca^{2+} and Mg^{2+} binding affinities, and thus determining its functional effects in cardiac myocytes. Specifically, compared to previously published studies, these experiments increase our understanding of how a Ca^{2+} buffering protein is able to increase contractility and highlight the importance of species/isoform-dependent effects in determining subcellular localization and effects on the Ca^{2+} transient. Taken together, the knowledge gained from this study contributes to the overall framework needed for strategic development of physiologically relevant Ca^{2+} buffers for the failing heart.

Mechanism of increased contractility with ParvE101D

The hypercontractile effect of ParvE101D is at least partially Ca^{2+} dependent, as evidenced by the corresponding increase in Ca^{2+} transient amplitude in paced myocytes. Free intracellular Ca^{2+} and Mg^{2+} have been implicated in the regulation of multiple Ca^{2+} handling proteins, including RyR2 (21–23), K_{ATP} (24), LTCC (25,26), and NCX (27). Additionally, altered Mg^{2+} concentration can affect myofilament function (28). The significantly greater increase in contraction amplitude with ParvE101D compared to ParvE101Q suggests that the greater Mg^{2+} affinity of ParvE101D contributes mechanistically to increased contractility. We speculate ParvE101D causes small, transient changes in localized Ca^{2+} and Mg^{2+} concentrations through Mg^{2+} release/Ca^{2+} binding during the relaxation phase and Ca^{2+} release/Mg^{2+} binding when the Ca^{2+} transient has terminated. These small changes in localized Ca^{2+} and Mg^{2+} may lead to altered function of proteins involved in CICR. The increase in spontaneous contractions in myocytes with ParvE101D led us to analyze Ca^{2+} sparks and Ca^{2+} waves as live cell functional measures of global intracellular Ca^{2+} handling. In our experiments, Ca^{2+} spark frequency was not changed, but spontaneous Ca^{2+} waves were significantly increased. The mechanism of increased Ca^{2+} waves in the absence of increased sparks is not known.

Species- and isoform-specific effects of parvalbumin function

To increase the translatability of Ca^{2+} buffering for the human heart, this study importantly made use of the human α-Parv isoform, whereas previously the carp β-Parv isoform was used (13). Although similar in tertiary structure, the two

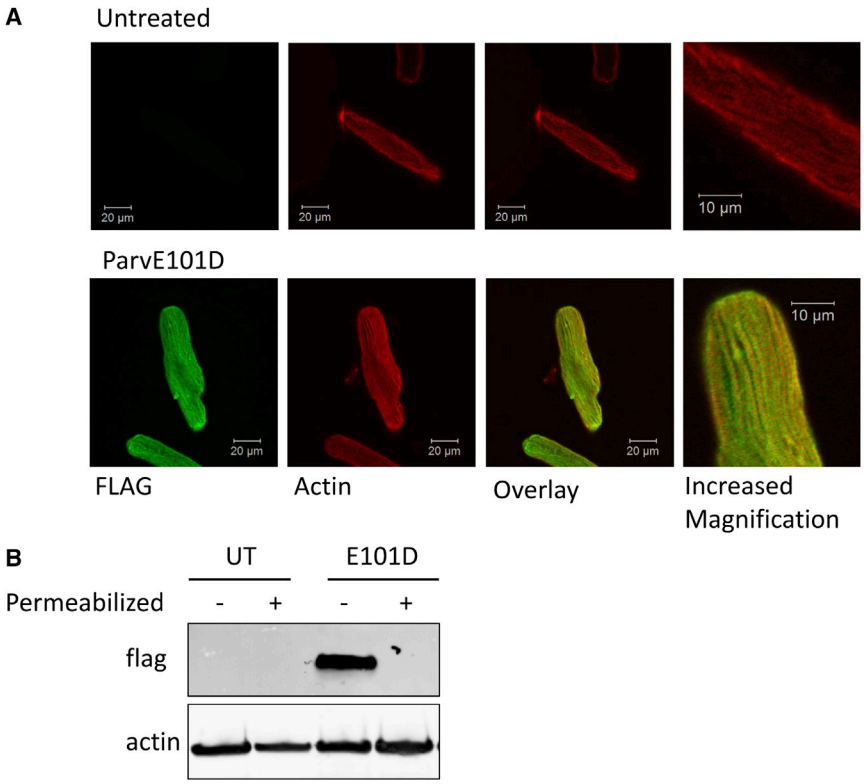

FIGURE 6 Subcellular localization of ParvE101D. (*A*) Representative immunofluorescence images of untreated myocytes and myocytes treated with ParvE101D. Images were obtained using confocal microscopy and a 63× oil objective. (*B*) Myocytes with and without ParvE101D were permeabilized with 0.1% Triton-X 100, washed, and then protein was probed for the presence of ParvE101D. UT, untreated myocytes.

proteins contain only 58% sequence homology. We found species/isoform-specific differences in subcellular localization patterns and Ca^{2+} transient effects. The increased Ca^{2+} transient amplitude caused by human α-ParvE101D and ParvE101Q in this study is in contrast to our previously published study on carp β-ParvE101Q, which reported a Ca^{2+}-independent increase in contractility (13). It is possible that different subcellular localization patterns between the two isoforms contributes to the mechanistic differences of enhanced contractile function. The different localization patterns are presumably the result of sequence differences between the isoforms, although this needs to be more thoroughly investigated in future studies.

In addition to the species/isoform-specific effects of Parv on Ca^{2+}/Mg^{2+} binding kinetics and buffering capacity, species differences in cardiac myocyte contraction/relaxation kinetics and Ca^{2+} cycling also likely has an effect on the functional effects of Parv expression. Although ParvE101D significantly increased contractility and modestly decreased relaxation time in the context of rat cardiac myocytes, the slower contraction/relaxation kinetics in the human heart may be more optimal for this ultra-delayed Ca^{2+} buffering protein. ParvE101D may buffer Ca^{2+} at a different stage of the human heart contraction/relaxation cycle, and, in this case, have a more robust effect on relaxation. These translational experiments in human heart or other large mammalian models with more human-like Ca^{2+} cycling kinetics will be important in the development of Ca^{2+} buffering as a therapeutic for human heart failure.

Mg^{2+} buffering

Total intracellular free Mg^{2+} concentrations are generally quite stable and highly buffered, making changes in Mg^{2+} difficult to study in the context of the intact cell. Total intracellular Mg^{2+} concentrations are between 17 and 20 mM and free Mg^{2+} is ~1 mM (29). Based upon estimated concentrations of virally transduced human α-Parv in cardiac myocytes from previous studies (9,18,30), the concentration of the high dose of ParvE101D used for most experiments in this study is estimated at 0.15–0.20 mM. This relatively small increase in Mg^{2+} buffering capacity in cardiac myocytes appears negligible in comparison to total cellular Mg^{2+}, but may be an important contributor to transient buffering of free Mg^{2+} during myocyte pacing in our experiments. In addition, the diffuse subcellular localization of ParvE101D around the Z-line may allow the formation of functionally relevant microdomains where ParvE101D is more concentrated and able to significantly buffer Mg^{2+} on a beat-to-beat basis during pacing. Indeed, restricted diffusion of cytosolic ions and proteins within cardiac myocytes, particularly near the sarcolemma, is an important contributor to spatiotemporal signaling (31). Indirect evidence for Mg^{2+} buffering as a mechanism of increased contractility in ParvE101D was shown by the contractility

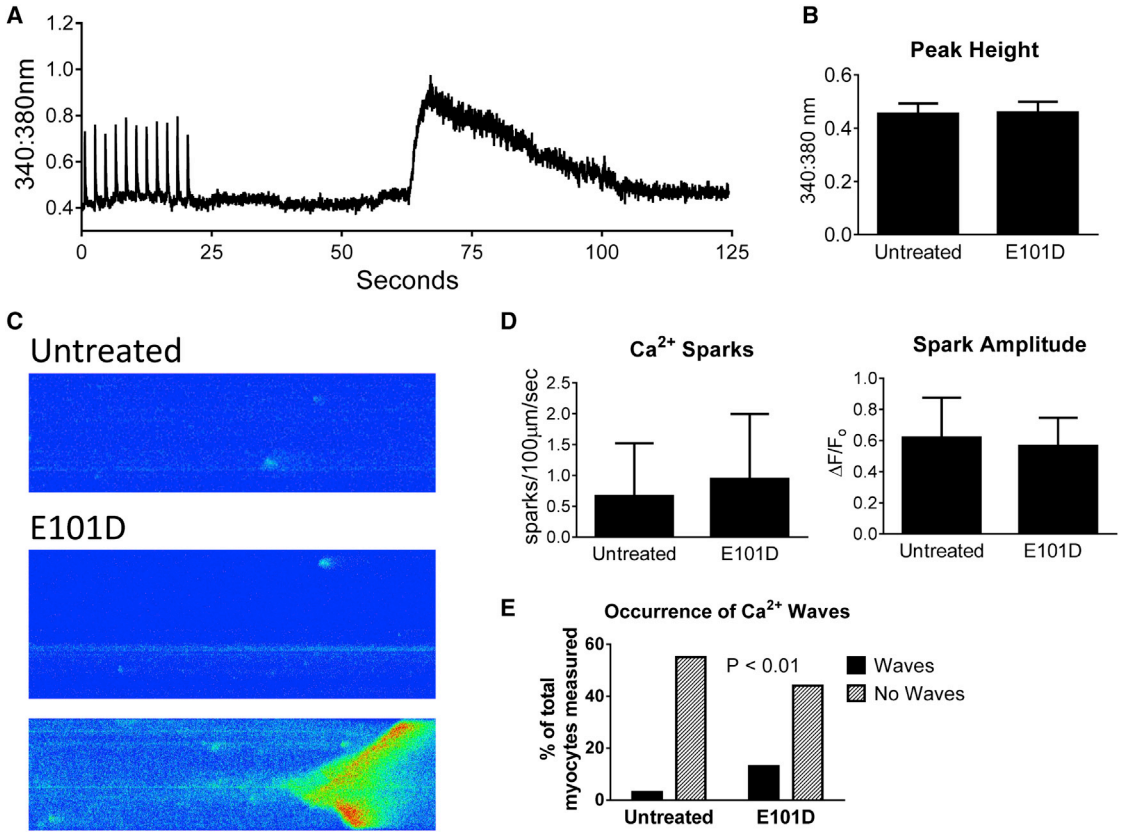

FIGURE 7 SR Ca^{2+} load, Ca^{2+} sparks, and waves with ParvE101D. (*A*) Representative trace and (*B*) peak height of caffeine-induced Ca^{2+} transients. Myocytes were tested at 30°C. Data are mean ± SE, $N = 16$ myocytes/group from four rats. (*C*) Representative images, (*D*) frequency and amplitude of Ca^{2+} sparks, and (*E*) occurrence of Ca^{2+} waves. Myocytes were tested at 30°C after pacing at 1 Hz for 20 s. Data are presented as median ± interquartile range in (*D*), $N = 159–167$ sparks and 57–58 myocytes from three rats.

changes that occurred acutely in untreated myocytes exposed to solutions with different Mg^{2+} concentrations. Although changes in localized intracellular Mg^{2+} concentration were not measured directly in our study, to our knowledge, this is the first study to provide evidence of the contractile effects of Mg^{2+} buffering in intact cardiac myocytes.

Structure-function of ParvE101D

Eliminating EF-hand loop residue 12 bidentate coordination of Ca^{2+} with a single E → D substitution elicited dramatic and opposing functional effects in cardiac myocytes. Canonical EF-hand binding loops, such as WT-Parv, bind Ca^{2+} with high affinity because of the ability of loop residue 12 to contribute both side-chain oxygen atoms to form the pentagonal bipyrimidal coordination sphere preferred by Ca^{2+}. Bidentate Ca^{2+} coordination by glutamate in ParvF102W and ParvD51A hastened relaxation at the expense of contractile function. Monodentate coordination by aspartate in ParvE101D decreased Ca^{2+} affinity and increased Mg^{2+} affinity, subsequently increasing contraction amplitude nearly 50% above that of untreated myocytes while minimally affecting relaxation. ~8% of EF-hand proteins in nature contain aspartate at position 12. These EF-hands are generally smaller and more compact in structure than parvalbumin so that the shorter aspartate side chain can form both monodentate and bidentate coordination (32,33). Crystallization studies and molecular dynamics simulations of Parv with an E → D substitution at loop residue 12 revealed that monodentate rather than bidentate coordination of Ca^{2+} occurred in the context of the larger binding loop. This preference occurred because of the rigidity of the tertiary structure and the required distance the F-helix would need to move for both side-chain oxygen atoms to be in coordinating distance to the Ca^{2+} ion (6,14).

CONCLUSIONS

In conclusion, we provide evidence that the inverted Ca^{2+}/Mg^{2+} binding affinities of human α-ParvE101D increase contraction amplitude in cardiac myocytes, and affect relaxation to a lesser extent. This study demonstrates that eliminating bidentate binding at EF-hand loop position 12 can elicit dramatic changes in myocyte contractile

function. Additionally, these data demonstrate there is a delicate balance between Ca^{2+}/Mg^{2+} binding affinities and dissociation rates that is required in designing a temporally optimized Ca^{2+} buffering system for human heart failure that both preserves contractile function and increases the rate of relaxation. Therefore, engineered ParvE101D provides mechanistic insight into the effects of Mg^{2+} buffering on rodent cardiac myocyte contractility. It will be important in future works to fully assess this and other EF-hand motifs in myocytes and hearts from larger mammals with Ca^{2+} handling properties more comparable to human heart.

AUTHOR CONTRIBUTIONS

M.L.A. designed and performed most of the experiments, analyzed data, and wrote the article; F.V.S. performed myocyte isolations, made viruses, and contributed to manuscript preparation; J.S. and J.D. made purified protein, performed in vitro binding assays, and contributed to manuscript preparation; J.M.M. directed and oversaw all aspects of the project, and contributed to writing the article.

ACKNOWLEDGMENTS

The authors thank Jenny Seong for her assistance with cloning, Lillehei Heart Institute for use of the confocal microscope, and Wang Wang and members of the J.M.M. lab for insightful discussions about the data.

This research was supported by funds from National Institutes of Health (NIH) to J.M.M. and by NIH National Heart, Lung, and Blood Institute (NHLBI) award 5F32HL115876 to M.L.A.

REFERENCES

1. Schwaller, B. 2009. The continuing disappearance of "pure" Ca2+ buffers. *Cell. Mol. Life Sci.* 66:275–300.
2. Pauls, T. L., J. A. Cox, and M. W. Berchtold. 1996. The Ca2+(−) binding proteins parvalbumin and oncomodulin and their genes: new structural and functional findings. *Biochim. Biophys. Acta.* 1306:39–54.
3. Kumar, V. D., L. Lee, and B. F. P. Edwards. 1990. Refined crystal structure of calcium-liganded carp parvalbumin 4.25 at 1.5-A resolution. *Biochemistry.* 29:1404–1412.
4. Gifford, J. L., M. P. Walsh, and H. J. Vogel. 2007. Structures and metal-ion-binding properties of the Ca2+-binding helix-loop-helix EF-hand motifs. *Biochem. J.* 405:199–221.
5. Permyakov, E. A. 2007. Parvalbumin. Nova Science Publishers, New York.
6. Cates, M. S., M. B. Berry, …, G. N. Phillips, Jr. 1999. Metal-ion affinity and specificity in EF-hand proteins: coordination geometry and domain plasticity in parvalbumin. *Structure.* 7:1269–1278.
7. Beuckelmann, D. J., M. Näbauer, and E. Erdmann. 1992. Intracellular calcium handling in isolated ventricular myocytes from patients with terminal heart failure. *Circulation.* 85:1046–1055.
8. Szatkowski, M. L., M. V. Westfall, …, J. M. Metzger. 2001. In vivo acceleration of heart relaxation performance by parvalbumin gene delivery. *J. Clin. Invest.* 107:191–198.
9. Coutu, P., and J. M. Metzger. 2005. Genetic manipulation of calcium-handling proteins in cardiac myocytes. I. Experimental studies. *Am. J. Physiol. Heart Circ. Physiol.* 288:H601–H612.
10. Asp, M. L., J. J. Martindale, …, J. M. Metzger. 2013. Calcium mishandling in diastolic dysfunction: mechanisms and potential therapies. *Biochim. Biophys. Acta.* 1833:895–900.
11. Coutu, P., and J. M. Metzger. 2005. Genetic manipulation of calcium-handling proteins in cardiac myocytes. II. Mathematical modeling studies. *Am. J. Physiol. Heart Circ. Physiol.* 288:H613–H631.
12. Zhang, J., V. Shettigar, …, J. P. Davis. 2011. Engineering parvalbumin for the heart: optimizing the Mg binding properties of rat β-parvalbumin. *Front. Physiol.* 2:77–85.
13. Wang, W., M. S. Barnabei, …, J. M. Metzger. 2013. Noncanonical EF-hand motif strategically delays Ca2+ buffering to enhance cardiac performance. *Nat. Med.* 19:305–312.
14. Cates, M. S., M. L. Teodoro, and G. N. Phillips, Jr. 2002. Molecular mechanisms of calcium and magnesium binding to parvalbumin. *Biophys. J.* 82:1133–1146.
15. 2005. Calcium phosphate - mediated transfection of eukaryotic cells. *Nat. Methods*. 2:319–320.
16. Asp, M. L., J. J. Martindale, and J. M. Metzger. 2013. Direct, differential effects of tamoxifen, 4-hydroxytamoxifen, and raloxifene on cardiac myocyte contractility and calcium handling. *PLoS One.* 8:e78768.
17. Picht, E., A. V. Zima, …, D. M. Bers. 2007. SparkMaster: automated calcium spark analysis with ImageJ. *Am. J. Physiol. Cell Physiol.* 293:C1073–C1081.
18. Coutu, P., and J. M. Metzger. 2002. Optimal range for parvalbumin as relaxing agent in adult cardiac myocytes: gene transfer and mathematical modeling. *Biophys. J.* 82:2565–2579.
19. Bassani, J. W., W. Yuan, and D. M. Bers. 1995. Fractional SR Ca release is regulated by trigger Ca and SR Ca content in cardiac myocytes. *Am. J. Physiol.* 268:C1313–C1319.
20. Bassani, J. W., R. A. Bassani, and D. M. Bers. 1994. Relaxation in rabbit and rat cardiac cells: species-dependent differences in cellular mechanisms. *J. Physiol.* 476:279–293.
21. Gusev, K., and E. Niggli. 2008. Modulation of the local SR Ca2+ release by intracellular Mg2+ in cardiac myocytes. *J. Gen. Physiol.* 132:721–730.
22. Laver, D. R., and B. N. Honen. 2008. Luminal Mg2+, a key factor controlling RYR2-mediated Ca2+ release: cytoplasmic and luminal regulation modeled in a tetrameric channel. *J. Gen. Physiol.* 132: 429–446.
23. Zahradníková, A., I. Valent, and I. Zahradník. 2010. Frequency and release flux of calcium sparks in rat cardiac myocytes: a relation to RYR gating. *J. Gen. Physiol.* 136:101–116.
24. Michailova, A., J. Saucerman, …, A. D. McCulloch. 2005. Modeling regulation of cardiac KATP and L-type Ca2+ currents by ATP, ADP, and Mg2+. *Biophys. J.* 88:2234–2249.
25. Brunet, S., T. Scheuer, and W. A. Catterall. 2009. Cooperative regulation of Ca(v)1.2 channels by intracellular Mg(2+), the proximal C-terminal EF-hand, and the distal C-terminal domain. *J. Gen. Physiol.* 134:81–94.
26. Wang, M., M. Tashiro, and J. R. Berlin. 2004. Regulation of L-type calcium current by intracellular magnesium in rat cardiac myocytes. *J. Physiol.* 555:383–396.
27. Wei, S. K., J. F. Quigley, …, M. C. P. Haigney. 2002. Cytosolic free magnesium modulates Na/Ca exchange currents in pig myocytes. *Cardiovasc. Res.* 53:334–340.
28. Smith, G. A., J. I. Vandenberg, N. S. Freestone, and H. B. F. Dixon. 2001. The effect of Mg 2 + on cardiac muscle function : is CaATP the substrate for priming myofibril cross-bridge formation and Ca 2 + reuptake by the sarcoplasmic reticulum? *Biochem. J.* 551: 539–551.
29. Romani, A. M. P. 2011. Cellular magnesium homeostasis. *Arch. Biochem. Biophys.* 512:1–23.
30. Rodenbaugh, D. W., W. Wang, …, J. M. Metzger. 2007. Parvalbumin isoforms differentially accelerate cardiac myocyte relaxation kinetics

in an animal model of diastolic dysfunction. *Am. J. Physiol. Heart Circ. Physiol.* 293:H1705–H1713.

31. Alekseev, A. E., S. Reyes, …, A. Terzic. 2012. Compartmentation of membrane processes and nucleotide dynamics in diffusion-restricted cardiac cell microenvironment. *J. Mol. Cell. Cardiol.* 52:401–409.

32. Cook, W. J., L. C. Jeffrey, …, S. Vijay-Kumar. 1993. Structure of a sarcoplasmic calcium-binding protein from amphioxus refined at 2.4 A resolution. *J. Mol. Biol.* 229:461–471.

33. Vijay-Kumar, S., and W. J. Cook. 1992. Structure of a sarcoplasmic calcium-binding protein from *Nereis diversicolor* refined at 2.0 A resolution. *J. Mol. Biol.* 224:413–426.